Low-frequency earthquakes in the Mexican Sweet Spot

William B. Frank, Nikolaï M. Shapiro, Vladimir Kostoglodov, Allen L. Husker, Michel Campillo, Juan S. Payero, Germán. A. Prieto

Low-frequency earthquakes in the Mexican Sweet Spot

William B. Frank,[1] Nikolaï M. Shapiro,[1] Vladimir Kostoglodov,[2] Allen L. Husker,[2]
Michel Campillo,[3] Juan S. Payero,[2] and Germán A. Prieto[4]

Received 15 April 2013; revised 12 May 2013; accepted 13 May 2013; published 13 June 2013.

[1] We use data from the Meso-America Subduction Experiment to detect and locate low-frequency earthquakes (LFEs) in the Mexican subduction zone. We use visually-identified templates to perform a network waveform correlation search that produced ~17,000 robustly detected LFEs that form 15 distinct families. Stacking an LFE family's corresponding detections results in seismograms with high signal-to-noise ratios and clear *P* and *S* wave arrivals; we use these travel times to locate the sources. The resulting locations superpose a previously identified region of permanent non-volcanic tremor (NVT) activity. Husker et al. (2012) called this region a Sweet Spot, suggesting that the local conditions are adequate to continuously generate NVT. The LFE hypocenters have been located at a depth of 40–45 km in an area that is surrounding the upper slab-plate interface. We characterize their focal mechanisms by comparing their stacked seismograms to synthetic seismograms. This analysis reveals a common low-dipping focal mechanism.
Citation: Frank, W. B., N. M. Shapiro, V. Kostoglodov, A. L. Husker, M. Campillo, J. S. Payero, and G. A. Prieto (2013), Low-frequency earthquakes in the Mexican Sweet Spot, *Geophys. Res. Lett.*, *40*, 2661–2666, doi:10.1002/grl.50561.

1. Introduction

[2] Nonvolcanic tremor (NVT) and slow-slip events (SSEs) are closely related subduction phenomena that have been observed within the frictional transition zones of a majority of the world's subduction zones [e.g. *Schwartz and Rokosky*, 2007]. Despite recently improving the epicentral precision of NVT sources [*Ghosh et al*., 2009], their origin depth is difficult to constrain due to their emergent arrivals. *Shelly et al*. [2007] proposed that NVT observed in Shikoku, Japan is the resulting seismic signal of a swarm of small-amplitude, short-duration, impulsive seismic events called low-frequency earthquakes (LFEs). Recent studies have since observed LFEs in northern Cascadia and northern Costa Rica, in addition to Southwestern Japan, and have proposed using LFEs as a proxy for NVT characterization [*Brown et al*., 2009; *Bostock et al*., 2012].

[3] There have also been observations of SSEs and NVTs in the Mexican subduction zone [*Larson et al*., 2007; *Payero et al*., 2008] (Figure 1). *Kostoglodov et al*. [2010] observed that SSEs and NVT do not originate in the same part of the transition zone in Mexico; there is, however, evidence of a temporal correlation between the two phenomena. More recently, precise epicentral locations of Mexican NVTs performed by *Husker et al*. [2012] showed that there are in fact two distinct NVT activity regimes in Mexico. In the downdip portion of the transition zone closer to the stable-slipping portion of the subduction interface, NVTs are observed more or less continuously and are punctuated every several months by high-energy NVT episodes (several NVTs observed together over a short time period on the order of several days). Farther updip, closer to the seismogenic zone, NVTs are only observed within episodes that occur due to transient stress induced by teleseismic earthquakes or SSEs. *Husker et al*. [2012] called the downdip region containing the continuously observed NVTs the NVT Sweet Spot and proposed that it is an area of the subduction interface that has the necessary conditions to more or less continuously generate NVTs. The regions that only produce NVT episodes are only conducive to NVT generation under strain induced by SSEs or by the arrival of seismic waves generated by large ($M_w > 7$) teleseismic earthquakes [*Zigone et al*., 2012].

[4] The Mexican subduction zone is an ideal region to study SSEs, NVTs, and LFEs due to the proximity of the Mexican coast to the subduction trench and the flat geometry of the subducting Cocos plate. These two features allow seismic networks to be installed directly above the region of interest, permitting robust observations of seismic events. The Meso-America Subduction Experiment (MASE) installed a dense (5–6 km spacing), linear network of broadband seismic stations between Acapulco and Tempoal (running through Mexico City, see Figure 1) from 2005 to mid-2007 that produced a high-quality data set intended to characterize the subduction geometry. The MASE network has since been used to characterize NVT in Mexico [*Husker et al*., 2012; *Kostoglodov et al*., 2010; *Payero et al*., 2008]. Using 10 broadband MASE stations that were chosen based on their high signal-to-noise ratios (SNR), their proximity to the NVT source region, and the continuity of their data sets, we report here the first observations of LFEs in the Mexican subduction zone. We then characterize their source locations and their focal mechanisms.

2. Detecting LFEs

[5] The LFEs we observed in the Mexican subduction zone are characterized principally by their small-amplitude,

Additional supporting information may be found in the online version of this article.

[1]Équipe de Sismologie, Institut de Physique du Globe de Paris, Paris Sorbonne Cité, CNRS, Paris, France.
[2]Instituto de Geofísica, Universidad Nacional Autónoma de México, México D. F., Mexico.
[3]Institut des Sciences de la Terre, Université Joseph Fourier, CNRS, IRD, Grenoble, France.
[4]Department of Earth, Atmospheric, and Planetary Sciences, Massachusetts Institute of Technology, Boston, Massachusetts, USA.

Corresponding author: W. B. Frank, Équipe de Sismologie, Institut de Physique du Globe de Paris, 1, rue Jussieu, Paris FR-75238, France. (frank@ipgp.fr)

0094-8276/13/10.1002/grl.50561

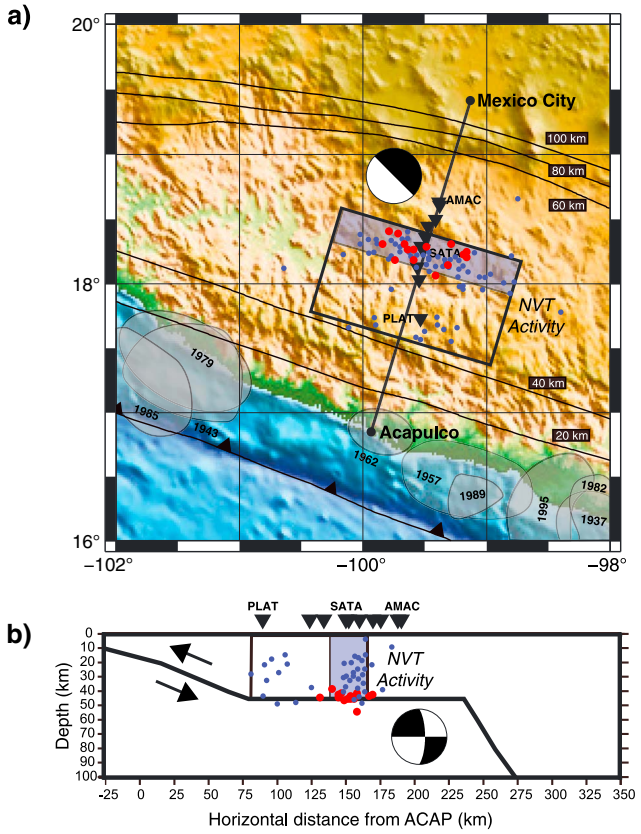

Figure 1. Nonvolcanic tremors (NVTs) and low-frequency earthquakes (LFEs) in Guerrero, Mexico. Blue circles are NVTs (observed between 2001 and 2007) located by *Payero et al*. [2008] using an envelope cross-correlation method [*Obara*, 2002]. Red circles are the 15 LFE family locations determined in this study. The black inverted triangles represent 10 broadband Meso-America Subduction Experiment (MASE) stations that operated between 2005 and mid-2007. The beach balls represent the stacked focal mechanism of the 15 LFE families projected into the respective planes of Figures 1a and 1b. The black box indicates the NVT source region determined by *Husker et al*. [2012] by inverting for NVT energy profiles with respect to the MASE network; the light blue shaded box indicates the Mexican Sweet Spot. The geometry of the top of the subducting Cocos slab is shown by the black contours and their associated depths in Figure 1a and by the solid black line in Figure 1b [*Kim et al*., 2010]. (a) Historical earthquakes (with rupture years) highlighting the Guerrero seismic gap are indicated by the gray shaded patches [*Kostoglodov and Pacheco*, 1999]. The black line between Acapulco and Mexico City indicates the location of the vertical profile in Figure 1b. (b) The arrows show the approximate direction of slip along the interface that releases accumulated tectonic stress.

impulsive arrivals within previously identified episodes of NVT. The pre-processing of our data consisted of removing the mean and the linear trend from each of our daily seismograms and then band-pass filtering between 1–2 Hz, as *Payero et al*. [2008] have observed this frequency band to have the highest SNR for Mexican NVT. This proved to be case as well for Mexican LFEs, as evidenced by Figure 3. The essential criteria when identifying LFEs by eye are coherent arrivals across several stations; the strongest LFE SNR, and by consequence the easiest identification, is on the horizontal components due to their principally shearing motions [*Husker et al*., 2012; *Kostoglodov et al*., 2010; *Payero et al*., 2008; *Shelly et al*., 2006].

2.1. Network Waveform Correlation Search

[6] The detection of LFEs in this study was performed using a network waveform correlation search based on the method developed by *Gibbons and Ringdal* [2006] and used by *Shelly et al*. [2007] to detect LFEs in Japan. Once an LFE template is identified within an NVT, it is used to scan for similar events within the MASE data set. A sliding window of the data set is compared to the LFE template by summing the correlation coefficients of each trace (CC sum). We used all three components (N–S, E–W, and vertical) of each analyzed MASE station simultaneously to compute the CC sum. All compared windows whose CC sums are larger than the detection threshold are considered multiplets of the LFE template (see the supporting information regarding our detection threshold of five times the RMS of the daily CC sum). Figure 2 shows an LFE multiplet detected by an LFE template and its corresponding spike in the daily CC sum. All of the detected multiplets then form the LFE family defined by the template used to perform the search.

2.2. Detection Robustness

[7] Due to the limited frequency band of investigation, there is a large risk of ambiguous detections and cycle-skipping while performing the network waveform correlation search. This could produce lengthy correlation envelopes with multiple strong correlations within a short-time window. We overcame this obstacle by developing a multi-frequency band CC sum analysis that was used to determine which of the detected LFE multiplets are robust detections. We consider a detection to be unambiguous (or robust) when the possibility of it being a cycle-skipped detection is adequately small. For a description of how detection's ambiguity is quantified, we refer the reader to the supporting information.

[8] We found that stacking only the robust detections produced as good or better quality stacks than stacks that were produced with the entire catalog of detections and often resulted in larger SNRs or the emergence of new phases that were previously buried in noise.

2.3. Stacking LFE Families

[9] After determining the family of robust detections similar to a given LFE template, they are stacked together to greatly increase the SNR. To further increase the SNR, a second network waveform correlation search was then performed with the LFE family's stack as its new template. This allowed us to significantly increase the number of detections, as shown in Table S2. While the length of the original LFE template could vary according to the event originally chosen by eye, the length of the second LFE template based on the initial stack was defined to be the same across all of the LFE families characterized in this study. We chose 18 s based on the asymptotic nature of the number of detected multiplets with increasing template length as computation time is directly proportional to template length (see Table S1).

[10] Not only does the resulting stack show clear *S* wave arrivals, but the increased SNR also allows *P* waves previously

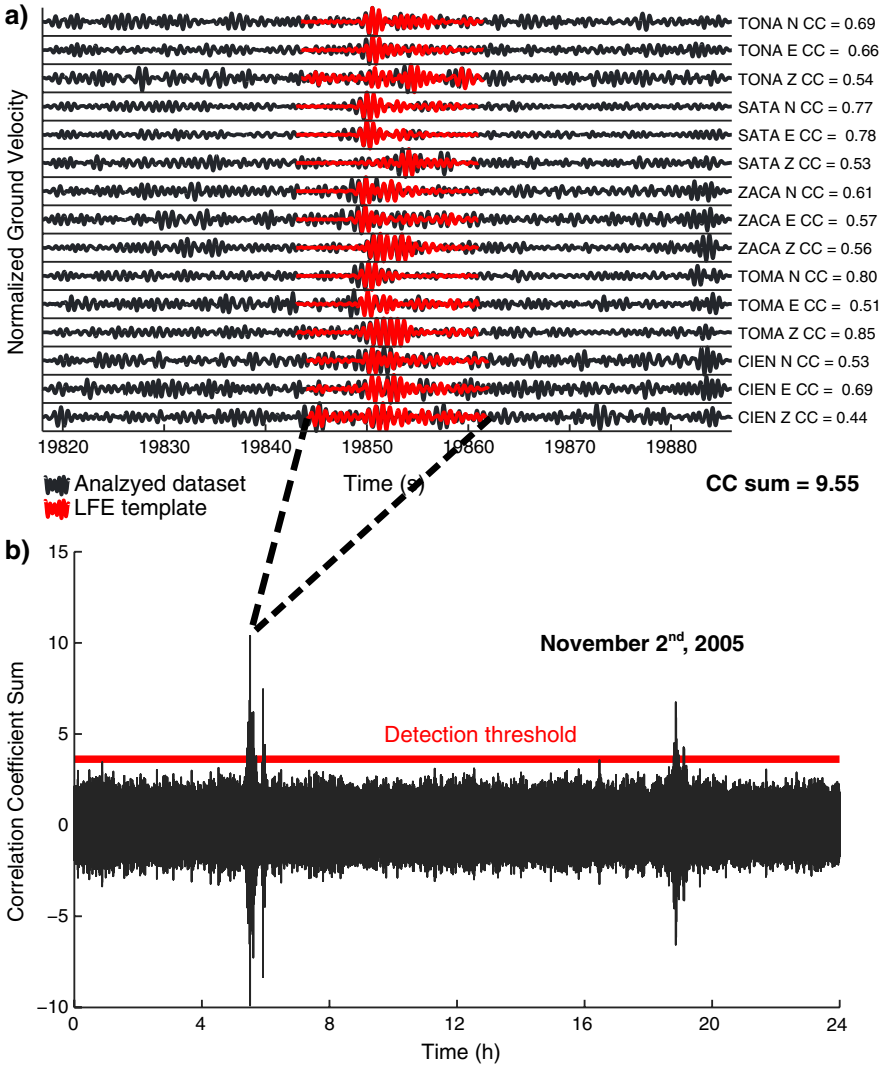

Figure 2. Detection of a low-frequency earthquake multiplet (LFE) on 2 November 2005 using the LFE template of family #3 chosen on 20 March 2005. (a) The correlation coefficients of an LFE template (in red) and the analyzed data set (in black) are shown to sum to a significant value. The station name and component are shown to the right of the seismograms with the corresponding correlation coefficient. The analyzed data set and the LFE template are shown in the highest signal-to-noise ratio frequency band (1–2 Hz). (b) The correlation coefficient sum (CC sum), shown in black, is calculated on a daily basis. The red line represents the detection threshold, set at five times the RMS of the daily CC sum. Whenever a CC sum for a given time is larger than the detection threshold, a detection is recorded.

hidden in the background noise to emerge. Figure 3 provides an example of an LFE family's final stack. The *P* wave moveout along with the *S-P* time delays makes precise locations possible.

3. Characterizing LFE Families

3.1. Source Location

[11] To locate the 15 LFE families detected in this study, we performed a 3-D spatial grid search comparing theoretical moveouts to the observed moveouts on a given LFE family's stack. Theoretical moveouts were calculated with a ray tracing method. The velocity model used in this study is based on the shear wave velocity model of *Iglesias et al*. [2010]; *P* wave velocities were consequently calculated with a constant $\frac{v_P}{v_S}$ ratio of 1.74 [*Huesca-Pérez and Husker*, 2012].

[12] The most likely source was determined by minimizing a summed L2 travel-time difference based on three travel-time differences which are picked on the stacked LFE family waveforms. The travel-time differences we used in this study are the *P* wave and *S* wave moveouts along with the *S-P* time delays. We refer the reader to the supporting information for a more in-depth description of the method used.

3.2. Focal Mechanism

[13] The focal mechanisms of our LFE families were determined by comparing synthetic seismograms generated at the LFE family's most likely source to the LFE family's stacked seismograms. The synthetic seismograms were generated using a wave number summation method [*Bouchon*, 1981]. We compared the windows of each phase (*P* and *S* waves) and each trace by calculating the amount of in-phase (or coherent) energy determined by the maximum value of their

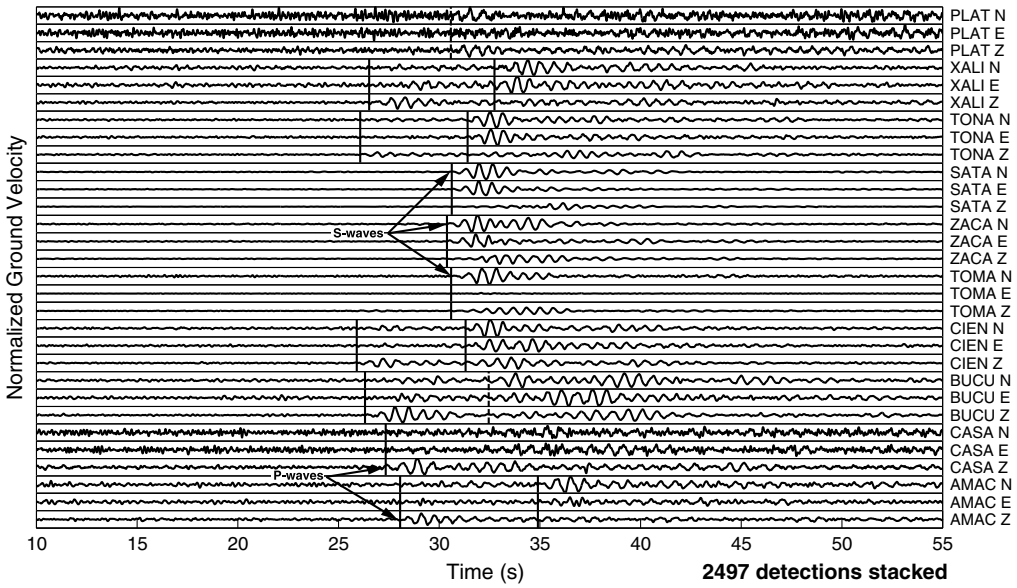

Figure 3. Stacked seismograms of 2497 robustly detected (of 7244 total) low-frequency earthquake (LFE) multiplets belonging to LFE family #3 chosen on 20 March 2005. The stacks were performed on 10 broadband Meso-America Subduction Experiment stations, from PLAT (the farthest south) to AMAC (the farthest north). The stacking process reveals *P* wave arrivals which are essential in precisely locating the LFE family's source (see Figures S3–S17 for all 15 LFE family source location misfit distributions). The stacked seismograms are filtered here between 1 and 6 Hz to highlight the dominant narrow frequency band of Mexican LFEs and are then normalized by station. Arrival picks are indicated by the black solid and dashed lines; dashed lines indicate lower confidence picks. No *P* wave arrivals can be observed on the three middle stations due to the LFE family's source location and the radiation pattern generated by the LFE family's focal mechanism (see Figure 1 and Figure S2).

cross-correlation function. Our method of calculating the coherent energy distribution of each LFE family is detailed in the supporting information.

[14] To evaluate the coherency of all of the LFE families' focal mechanisms, we stacked their normalized coherent energy distributions. The focal mechanism coherent energy stack of the 15 LFE families observed in this study robustly converges to a single shallow-thrusting double-couple mechanism (see Figure S2b for the stacked coherent energy distribution).

4. Results

[15] We characterized 15 different observed LFE families that are made up of ~17,000 robust detections (of ~54,000

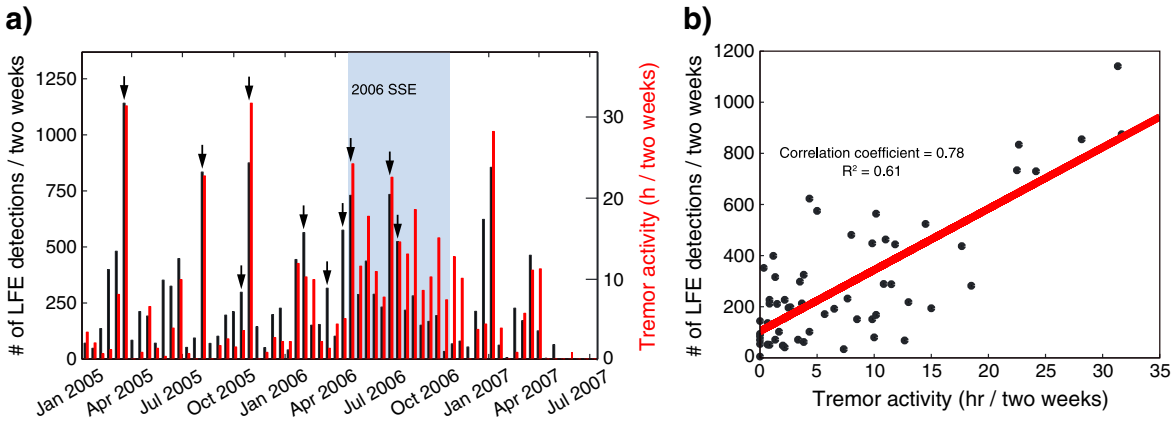

Figure 4. Temporal distribution of the robust low-frequency earthquake (LFE) multiplets from the 15 LFE families observed in this study during the Meso-America Subduction Experiment deployment (2005–mid-2007) and their correlation with non-volcanic tremor (NVT) activity [*Husker et al.*, 2010]. (a) The arrows indicate the dates when our 15 LFE templates were chosen. The activity of LFEs during the MASE deployment is more or less continuous with more multiplets being detected during periods of stronger NVT activity. Certain NVT episodes toward the end of the 2006 SSE do not coincide with LFE activity which is most likely due to a lack of LFE templates chosen during the SSE. (b) The red line represents the least mean-squares linear trend between the number of detected LFEs and NVT activity. The R^2 value indicates the amount of the variance that is explained by the linear trend, 1 indicating 100% of the variance and 0 indicating 0% of the variance.

total) detected over the entire MASE deployment that lasted two and a half years. The amount of robust detections per LFE family varied between 500 and 3000. Each family's distribution of detections in time covers the majority of the MASE deployment as shown in Figure 4a. Additionally, the total distribution of LFE detections is strongly correlated with NVT activity observed by *Husker et al*. [2010] as shown in Figure 4b. There are certain NVT episodes, however, principally occurring toward the end of the 2006 SSE, that are not observed with an accompanying increase of LFE detections. First, we believe to have only characterized a small portion of the regional LFE sources and this leaves the strong possibility that many LFEs that make up these "lone" NVTs have yet to be observed. Second, the majority of our LFE templates were identified and chosen before the 2006 SSE, greatly reducing the chance of detecting SSE-induced NVTs that originate in the updip portion of the transition zone.

[16] All of the LFE families' sources located to an area surrounding the plate interface in the farther downdip region of the Mexican subduction's transition zone as shown by the red circles in Figure 1; the source region superposes the deeper portion of the NVT Sweet Spot of *Husker et al*. [2012]. The misfit distributions of the source grid searches consistently showed strong, punctual minima with uncertainties on the order of 2–4 km (see Figures S3–S17 for the misfit distributions for all 15 LFE families).

[17] The focal mechanism coherent energy stack demonstrates that the focal mechanism of the majority of the observed LFE families is represented by a double couple moment tensor that reflects the first-order release of stress of the Mexican subduction zone. The inherent ambiguity of such a focal mechanism is demonstrated by the multiple maxima in the coherent energy distribution (see Figure S2).

5. Discussion

[18] We have observed LFEs within NVT in the Mexican subduction zone. The LFE multiplets that were detected using a network waveform correlation search were sorted by ambiguity so that the resulting stack only incorporated unambiguous detections; this sometimes even revealed new phases in the stacked waveforms when compared to stacking the entire catalog of detections.

[19] The LFE families characterized in this study locate near to the subduction interface and their common focal mechanism suggests a very shallow-dipping thrust fault. The activity of NVT in the region correlates well in time with our complete LFE catalog, indicating a link between the two phenomena. Our findings are similar to those from other studies that have characterized LFEs in other subduction zones and have provided evidence that LFEs are small thrust events that occur near the subduction interface that release accumulated tectonic stress [*Bostock et al*., 2012; *Ide et al*., 2007; *Ohta and Ide*, 2011; *Shelly et al*., 2007]. The Mexican LFEs are however lower dipping than the LFEs observed in Cascadia or Japan, reflecting the near-horizontal geometry of the subduction interface within the frictional transition zone [*Bostock et al*., 2012; *Ide et al*., 2007].

[20] The generation of NVT and LFEs and their relationship to SSEs is still not well understood. The buildup of pore pressure due to strong permeability contrasts at the Moho, influencing the rheological properties around the subduction interface, and the dehydration of the subducting slab through serpentinization and eclogitization were suggested as important factors in generating NVT and SSEs [*Audet et al*., 2009; *Katayama et al*., 2012; *Peacock et al*., 2011]. An ultra-slow velocity layer (USL) has been observed above several subduction zone interfaces that indicate a similar mechanism, greatly reducing the effective normal pressure around the interface [*Audet et al*., 2009; *Song et al*., 2009]. In Mexico, the USL extends up until the Sweet Spot, but does not extend into it; the lack of the USL within the Sweet Spot is perhaps due to the higher temperatures at the boundary of stable slipping and the onset of eclogitization [*Song et al*., 2009; *Audet et al*., 2009]. The near-constant generation of LFEs and NVTs in the Mexican Sweet Spot could therefore be explained by the absence of the USL and the consequent reduction in pore pressure [*Bostock et al*., 2012]. This is in accordance with recent studies that proposed that NVTs are generated at boundaries between different frictional regimes [*Walter et al*., 2011; *Wech and Creager*, 2011].

[21] These various pieces of evidence justify the separation of the NVT source regions in Mexico: the distribution of normal stress at the plate interface is not uniform across the entire transition zone and therefore while the downdip region of the transition zone (at the boundary of a stable-slipping regime) may have the conditions necessary to spontaneously generate NVT (the Sweet Spot), an additional forcing (such as SSEs) is needed to generate NVTs in the updip portion of the transition zone (at the boundary of a stick-slip regime) [*Husker et al*., 2012; *Wech and Creager*, 2011]. Our detection distribution in time, the source locations of the 15 observed LFE families, and the strong correlation found between LFEs and NVTs confirm that Sweet Spot NVT in Mexico is generated more or less continuously without any apparent large-scale forcings, reflecting the unique conditions of the subduction interface at a boundary between two frictional regimes.

6. Conclusions

[22] We have reported here the first observations of LFEs in the Mexican subduction zone. Using a network waveform correlation search with the MASE data set, we detected ~17,000 robust LFE multiplets that were used to form 15 distinct LFE families. After analyzing the catalog of detections using our proposed multi-band CC sum method, we were able to determine which detections were not ambiguous. This yielded high-quality stacked waveforms with clear *P* and *S* wave arrivals that provided precise hypocentral locations and focal mechanisms.

[23] The temporal distribution of the Mexican LFE detections shows that, similar to NVTs in the Sweet Spot [*Husker et al*., 2012], they occur more or less continuously. This is further confirmed by the strong temporal correlation between the two phenomena. The source locations of our 15 LFE families overlap the deeper portion of the Sweet Spot NVT region of the Mexican subduction's frictional transition zone along the subduction interface. The common focal mechanism found between a large majority of the 15 families indicates a horizontal thrusting moment tensor that reflects the geometry of the subduction interface within the Sweet Spot and matches the stress release of the subduction deformation regime.

[24] **Acknowledgments.** We thank the California Institute of Technology for the Meso-American Subduction Experiment data set used in this study. We also thank Aldo Zollo and Claudio Satriano for their program that was used to calculate the theoretical travel times. This work was supported by the Agence Nationale de la Recherche (France) under the contract RA0000CO69 (G-GAP), by the European Research Council under the contract FP7 ERC Advanced grant 227507 (WHISPER), and by the PAPIIT 110611–3 grant (UNAM Mexico). Several figures were made with Generic Mapping Tools [*Wessel and Smith*, 1998].

[25] The Editor thanks Michael Bostock and an anonymous reviewer for their assistance in evaluating this paper.

References

Audet, P., M. G. Bostock, N. I. Christensen, and S. M. Peacock (2009), Seismic evidence for overpressured subducted oceanic crust and megathrust fault sealing, *Nature*, *457*, 76–78.

Bostock, M. G., A. A. Royer, E. H. Hearn, and S. M. Peacock (2012), Low frequency earthquakes below southern Vancouver Island, *Geochem. Geophys. Geosyst.*, *13*, Q11007, doi:10.1029/2012GC004391.

Bouchon, M. (1981), A simple method to calculate Green's functions for elastic layered media, *Bull. Seismol. Soc. Am.*, *71*(4), 959–971.

Brown, J. R., G. C. Beroza, S. Ide, K. Ohta, D. R. Shelly, S. Y. Schwartz, W. Rabbel, M. Thorwart, and H. Kao (2009), Deep low-frequency earthquakes in tremor localize to the plate interface in multiple subduction zones, *Geophys. Res. Lett.*, *36*, L19306, doi:10.1029/2009GL040027.

Ghosh, A., J. E. Vidale, J. R. Sweet, K. C. Creager, and A. G. Wech (2009), Tremor patches in Cascadia revealed by seismic array analysis, *Geophys. Res. Lett.*, *36*, L17316, doi:10.1029/2009GL039080.

Gibbons, S. J., and F. Ringdal (2006), The detection of low magnitude seismic events using array-based waveform correlation, *Geophys. J. Int.*, *165*, 149–166.

Huesca-Pérez, E., and A. L. Husker (2012), Shallow travel-time tomography below southern Mexico, *Geofis. Int.*, *51*(3), 281–291.

Husker, A. L., S. Peyrat, N. M. Shapiro, and V. Kostoglodov (2010), Automatic non-volcanic tremor detection in the Mexican subduction zone, *Geofis. Int.*, *49*, 17–25.

Husker, A. L., V. Kostoglodov, V. M. Cruz-Atienza, D. Legrand, N. M. Shapiro, J. S. Payero, M. Campillo, and E. Huesca-Pérez (2012), Temporal variations of non-volcanic tremor (NVT) locations in the Mexican subduction zone: Finding the NVT sweet spot, *Geochem. Geophys. Geosyst.*, *13*, Q03011, doi:10.1029/2011GC003916.

Ide, S., D. R. Shelly, and G. C. Beroza (2007), Mechanism of deep low frequency earthquakes: Further evidence that deep non-volcanic tremor is generated by shear slip on the plate interface, *Geophys. Res. Lett.*, *34*, L03308, doi:10.1029/2006GL028890.

Iglesias, A., R. W. Clayton, X. Pérez-Campos, S. K. Singh, J. F. Pacheco, D. García, and C. Valdés-González (2010), S wave velocity structure below central Mexico using high-resolution surface wave tomography, *J. Geophys. Res.*, *115*, B06307, doi:10.1029/2009JB006332.

Katayama, I., T. Terada, K. Okazaki, and W. Tanikawa (2012), Episodic tremor and slow slip potentially linked to permeability contrasts at the Moho, *Nat. Geosci.*, *5*, 731–734.

Kim, Y. H., R. W. Clayton, and J. M. Jackson (2010), Geometry and seismic properties of the subducting Cocos plate in central Mexico, *J. Geophys. Res.*, *115*, B06310, doi:10.1029/2009JB006942.

Kostoglodov, V., and J. F. Pacheco, (1999), Cien años de sismicidad en México, Instituto de Geofísica, Universidad Nacional Autónoma de México, http://usuarios.geofisica.unam.mx/vladimir/sismos/100a%F1os.html.

Kostoglodov, V., A. L. Husker, N. M. Shapiro, J. S. Payero, M. Campillo, N. Cotte, and R. W. Clayton (2010), The 2006 slow slip event and nonvolcanic tremor in the Mexican subduction zone, *Geophys. Res. Lett.*, *37*, L24301, doi:10.1029/2010GL045424.

Larson, K. M., V. Kostoglodov, S. Miyazaki, and J. A. S. Santiago (2007), The 2006 aseismic slow slip event in Guerrero, Mexico: New results from GPS, *Geophys. Res. Lett.*, *34*, L13309, doi:10.1029/2007GL029912.

Obara, K. (2002), Nonvolcanic deep tremor associated with subduction in southwest Japan, *Science*, *296*(5573), 1679–1681.

Ohta, K., and S. Ide (2011), Precise hypocenter distribution of deep low-frequency earthquakes and its relationship to the local geometry of the subducting plate in the Nankai subduction zone, Japan, *J. Geophys. Res.*, *116*, B01308, doi:10.1029/2010JB007857.

Payero, J. S., V. Kostoglodov, N. M. Shapiro, A. Iglesias, X. Pérez-Campos, and R. W. Clayton (2008), Nonvolcanic tremor observed in the Mexican subduction zone, *Geophys. Res. Lett.*, *35*, L07305, doi:10.1029/2007GL032877.

Peacock, S. M., N. I. Christensen, M. G. Bostock, and P. Audet (2011), High pore pressures and porosity at 35 km depth in the Cascadia subduction zone, *Geology*, *39*, 471–474.

Schwartz, S. Y., and J. M. Rokosky (2007), Slow slip events and seismic tremor at circum-Pacific subduction zones, *Rev. Geophys.*, *45*, RG3004, doi:10.1029/2006RG000208.

Shelly, D. R., G. C. Beroza, and S. Ide (2006), Low-frequency earthquakes in Shikoku, Japan, and their relationship to episodic tremor and slip, *Nature*, *442*, 188–191.

Shelly, D. R., G. C. Beroza, and S. Ide (2007), Non-volcanic tremor and low-frequency earthquake swarms, *Nature*, *446*, 305–307.

Song, T.-R. A., D. V. Helmberger, M. R. Brudzinski, R. W. Clayton, P. M. Davis, X. Pérez-Campos, and S. K. Singh (2009), Subducting slab ultra-slow velocity layer coincident with silent earthquakes in southern Mexico, *Science*, *324*, 502–506.

Walter, J. I., S. Y. Schwartz, J. M. Protti, and V. Gonzalez (2011), Persistent tremor within the northern Costa Rica seismogenic zone, *Geophys. Res. Lett.*, *38*, L01307, doi:10.1029/2010GL045586.

Wech, A. G., and K. C. Creager (2011), A continuum of stress, strength and slip in the Cascadia subduction zone, *Nature Geoscience*, *4*, 624–628 doi:10.1038/ngeo1215.

Zigone, D., D. Rivet, M. Radiguet, M. Campillo, C. Voisin, N. Cotte, A. Walpersdorf, N. M. Shapiro, G. Cougoulat, and P. Roux (2012), Triggering of tremors and slow slip event in Guerrero, Mexico, by the 2010 Mw 8.8 Maule, Chile, earthquake, *J. Geophys. Res.*, *117*, B09304, doi:10.1029/2012JB009160.